Development 140, 413-422 (2013) doi:10.1242/dev.082578

Bridging Decapentaplegic and Wingless signaling in *Drosophila* wings through repression of *naked cuticle* by Brinker

Lin Yang, Fei Meng*, Da Ma, Wei Xie and Ming Fang‡

SUMMARY

Wnts and bone morphogenetic proteins (BMPs) are signaling elements that are crucial for a variety of events in animal development. In *Drosophila*, Wingless (Wg, a Wnt ligand) and Decapentaplegic (Dpp, a BMP homolog) are thought to function through distinct signal transduction pathways and independently direct the patterning of the wing. However, recent studies suggest that Mothers against Dpp (Mad), the key transducer of Dpp signaling, might serve as a node for the crosstalk between these two pathways, and both positive and negative roles of Mad in Wg signaling have been suggested. Here, we describe a novel molecular mechanism by which Dpp signaling suppresses Wg outputs. Brinker (Brk), a transcriptional repressor that is downregulated by Dpp, directly represses *naked cuticle* (*nkd*), which encodes a feedback inhibitor of Wg signaling, *in vitro* and *in vivo*. Through genetic studies, we demonstrate that Brk is required for Wg target gene expression in fly wing imaginal discs and that loss or gain of *brk* during wing development mimics loss or gain of Wg signaling, respectively. Finally, we show that Dpp positively regulates the expression of *nkd* and negatively regulates the Wg target gene *Distal-less* (*Dll*). These data support a model in which different signaling pathways interact via a negative-feedback mechanism. Such a mechanism might explain how organs coordinate inputs from multiple signaling cues.

KEY WORDS: BMP, Brk, *Drosophila*, Nkd, Wnt

INTRODUCTION

During animal development, proper organogenesis is achieved by simultaneous actions of highly conserved signaling pathways. One of the best-studied examples is the *Drosophila* imaginal discs, in which multiple signaling molecules, including Wg and Dpp, function as organizational cues to guide patterning. Both Wg and Dpp are thought to act as morphogens that activate a set of pathway-specific target genes in a gradient-dependent manner (Cadigan, 2002; Tabata and Takei, 2004). For instance, Wg target genes are predominantly regulated by the Wnt response elements (WREs) occupied by the transcription factor T cell factor (TCF; Pan – FlyBase) (for a review, see Cadigan, 2012). Wg signal transduction is centered around the stability of the cytosolic pool of Armadillo (Arm, the *Drosophila* homolog of β-catenin). Wg stabilizes Arm, causing its cytosolic accumulation and translocation into the nucleus, where Arm displaces co-repressors such as Groucho (Gro) and binds to TCF (Cadigan, 2012). This switches the TCF complex from a repressor to a transcriptional activator and turns on Wg target gene expression. In the case of Dpp target gene activation, two mechanisms have been proposed (for reviews, see Affolter et al., 2001; Affolter and Basler, 2007). In the first, Dpp-dependent receptor activation induces phosphorylation of Mad, which then forms a heteromeric complex with Medea (Med) in the nucleus and functions as a sequence-specific activator (Wisotzkey et al., 1998). Alternatively, Dpp signaling can act by inhibiting Brk, a transcriptional repressor (Campbell and Tomlinson, 1999; Jaźwińska et al., 1999; Minami et al., 1999). This model has been well addressed in the developing fly wing, in which *dpp* is expressed in a narrow stripe across the anterior/posterior (A/P) boundary. *brk* is repressed in a dose-dependent manner by Dpp through a Schnurri-Mad-Med repressing complex and is expressed in complement with the Dpp gradient (Müller et al., 2003). Brk thus acts as a major interpreter of Dpp signaling in wing discs.

Developmental signaling pathways are often regulated by negative-feedback regulators, thus limiting their range of actions. Such regulation contributes to the refinement of target gene expression in cells receiving multiple signaling cues (Gerlitz and Basler, 2002; Chang et al., 2008a). *nkd*, expression of which is universally induced by Wg, is one such feedback inhibitor of Wg signaling in flies (Zeng et al., 2000). Nkd interacts directly with Dishevelled (Dsh) to antagonize Wnt signal transduction (Rousset et al., 2001), suggesting that *nkd* functions mainly to limit Wg activity in order to achieve proper activation of Wg target genes.

In general, crosstalk between signaling pathways ensures the proper balance of signaling during development. A notable example of this is in fly leg discs, in which Wg and Dpp signaling mutually repress each other to specify ventral and dorsal leg fates, respectively (Brook and Cohen, 1996; Jiang and Struhl, 1996; Johnston and Schubiger, 1996; Morimura et al., 1996; Penton and Hoffmann, 1996; Theisen et al., 1996; Morata, 2001). In addition, Wg and Dpp are both required for cell fate specification along the proximal/distal axis via direct activation of *Dll*, precise expression of which is crucial for leg development (Estella et al., 2008). In the wing disc, *wg* and *dpp* are expressed in perpendicular narrow stripes along the dorsal/ventral (D/V) and A/P boundaries, respectively. Unlike in leg discs, where *wg* and *dpp* are expressed in distinct domains, these two signaling molecules share a common expression pattern in the center of the wing pouch. Recent studies

Institute of Life Sciences, MOE Key Laboratory of Developmental Genes and Human Diseases, Southeast University, Nanjing 210096, China.

*Present address: Department of Clinical Laboratory, The Traditional Chinese Medicine Hospital of Jiangsu Province, Nanjing 210029, China
‡Author for correspondence (mfang@seu.edu.cn)

Accepted 5 November 2012

have suggested that Mad, one of the key transducers in Dpp signaling, might play a role in the Wg pathway in the wing. One study suggests that Mad and Arm compete for binding to TCF, with Mad serving as an intermediate through which Dpp signaling suppresses the Wg pathway (Zeng et al., 2008). Other studies, however, propose an alternative model in which Mad is required for both Wg and Dpp signal transduction depending on its phosphorylation status (Eivers et al., 2009; Eivers et al., 2011).

In this article, we uncover an additional level of Wg-Dpp crosstalk involving Nkd, a feedback inhibitor of Wg signaling, and Brk, the major transcriptional repressor for Dpp target genes. We show that Brk directly represses *nkd in vitro* and *in vivo*. The biological relevance of such regulation is exemplified in fly wing discs, where *brk* is required for proper expression of Wg targets in the presumptive hinge region, coincident with the fact that *brk* is expressed at the highest level in this area. In adult wing, altering *brk* levels gives rise to phenotypes similar to the gain and loss of Wg activities. Moreover, activation of Dpp signaling reduces Dll levels and increases *nkd* expression. Taken together, our data support a novel model in which Dpp signaling inhibits Wg outputs through a *brk-nkd* negative regulatory circuit.

MATERIALS AND METHODS

Drosophila genetics

All lines were cultured with standard medium at 25°C. *brk* somatic clones were generated exactly as described (Schwank et al., 2008). P[*UAS-brk*] (Jaźwińska et al., 1999), P[*UAS-nkd*] (Zeng et al., 2000), P[*UAS-tkv*^{QD}] (Nellen et al., 1996) and P[*UAS-TCFΔN*] (van de Wetering et al., 1997) were used in the overexpression experiments. P[*UAS-brk*^{RNAi}] (VDRC# GD2919, KK101887) and P[*UAS-nkd*^{RNAi}] (VDRC# GD3005) lines were obtained from the Vienna *Drosophila* RNAi Center. Experiments with *En-Gal4* and *Vg-Gal4* were carried out at 25°C, whereas those with *Ptc-Gal4* were carried out at 20°C. For temporal ectopic expression of *brk* and *tkv*^{QD} driven by *En-Gal4*, P[*UAS-brk*] and P[*UAS-tkv*^{QD}] were crossed with P[*En-Gal4*], P[*tubP-Gal80*^{ts}], P[*UAS-GFP*] line, and the progenies were shifted to a restrictive temperature at 29°C from the second instar larval stage and thereafter (Schwank et al., 2008). For heat-shock induction of *tkv*^{QD}, P[*Hsp70-Gal4*]/P[*UAS-tkv*^{QD}] third instar larvae were heat shocked at 37°C for 1 hour, once a day for 2 days, and total RNAs were extracted from young adult flies 4 days after eclosion. For *Nkd-lacZ* reporter expression, we used a line containing both upstream and intron WREs of *nkd* as described (Chang et al., 2008a).

Antibodies

Rabbit polyclonal anti-Brk antiserum was generated against a Brk fragment (361-619 aa). For western blot analyses, anti-Brk (1:5000), anti-Tubulin (1:5000, Sigma) or anti-Flag (1:5000) antibodies were used. Immunostaining of imaginal discs was performed as described (Fang et al., 2006) using the following antibodies: anti-Dll (1:500) (Panganiban et al., 1995), anti-Sens (1:1000) (Nolo et al., 2000) and anti-Wg (1:200, Developmental Studies Hybridoma Bank at the University of Iowa, USA).

Electrophoretic mobility shift assay (EMSA)

EMSA was performed with a Lightshift Chemiluminescent EMSA Kit (Thermo Scientific) according to the manufacturer's instructions. For production of recombined GST-BrkDBD, a cDNA fragment encoding 44-99 amino acid residues of Brk (Saller et al., 2002; Cordier et al., 2006) was expressed in *Escherichia coli* BL21 and affinity purified. The probe sequences were 5′-acaaaacgctttgtcggtcattagctttgagtggacgccg-3′ for wild type and 5′-acaaaacgctttgtcggtcattagctttgagtgtcagccg-3′ for the mutant form.

Kc cells culture, RNAi knockdown, real-time quantitative PCR (qPCR) and reporter assay

Kc167 (Kc) cells were routinely cultured in the Schneider's *Drosophila* media (Life Technologies) containing 5% FBS (Life Technologies) at 25°C. RNAi-mediated gene knockdown was performed as described (Worby et al., 2001). Double-stranded RNAs (dsRNAs) for control and *gro* were synthesized as described (Fang et al., 2006), and the dsRNA primer corresponding to *brk* were 5′-gaattaatacgactcactatagggagaaatttcaagcggc-ccaaggattcttcg-3′ and 5′-gaattaatacgactcactatagggagatgttgctccttctgatg-ctgcatttgagg-3′. A million cells were cultured in serum-free medium for 1 hour, 9 μg of a mixture of two dsRNAs (combination indicated in Fig. 1A, or the indicated one plus the control dsRNA) was added, and FBS was supplemented to reach a final concentration of 5%. Total RNAs were isolated 4 days later using the RNeasy Mini Kit (Qiagen), and 2 μg of each sample was reverse transcribed with a superscript III reverse transcriptase (Life Technologies). qPCR assays were performed with Applied Biosystems 7300 Real-Time PCR System (Life Technologies). qPCR detections for *wg* and *brk* were carried out with a FastStart Universal SYBR Green Master Mix (Roche Applied Science). The primer pairs were for *wg*, 5′-cgtcagggacgcaagcata-3′ and 5′-attgtgcgggttcagttgg-3′; for *brk*, 5′-tcgggagctttgaatttcaag-3′ and 5′-tggctgtttgtggcattctc-3′. *nkd* qPCR was performed with FastStart TaqMan Probe Master (Roche Applied Science). The primer pairs and probe used were 5′-cgcatccgactggaggaa-3′, 5′-ggtcgtagaacgtgaacgagaac-3′ and 5′-FAM-tcacctgcgacgtgtccgtgg-BHQ1-3′. For *nkd* qPCR analysis in wing discs, total RNAs were extracted from 30 wing discs of third instar larvae using the RNeasy Micro Kit (Qiagen).

The reporter gene assay was performed as previously described (Fang et al., 2006; Chang et al., 2008a), except that pArm-Arm* and pArm-*lacZ* instead of pAc vectors were used. Reporter constructs were generated as previously described (Chang et al., 2008a). For IntE1200, primers 5′-agctcacgcgtgctctcgggccacttcttggaa-3′ and 5′-cgcatcccggggcctgccactttg-cttcagtgaga-3′, with underlined bases indicating introduced restriction sites, were used to amplify the intronic region of *nkd*, and subcloned into a pGL3 (Promega) vector upstream to a *hsp70* minimal promoter (Chang et al., 2008a). IntE255 was as described (Chang et al., 2008a). IntE255^{Brkmut} were generated by PCR-introduced base substitutions that were the same as in the mutant probe in the EMSA assay. pAc-Brk-2XFlag was made from insertion of a PCR-amplified full-length coding sequence of *brk* plus two Flag tags into pAc5.1 (Life Technologies).

Transient transfections were carried out with Fugene HD (Roche Applied Science) according to the manufacturer's instructions. A plasmid mixture containing 100 ng reporter, 1 ng pArm-*lacZ*, 10 ng pArm-Arm* and 10-80 ng pAc-Brk-2XFlag were co-transfected into a million cells. The empty pAc5.1 vector was used to normalize the DNA content or as a control. For experiments with RNAi followed by reporter assay, a million cells were incubated with 9 μg control or *brk* dsRNA for 2 days, washed with PBS twice and then transfected with pArm-*lacZ* (1 ng) and pArm-Arm* (10 ng). Luciferase and β-galactosidase activities were assayed 2 days after transfection, using the Tropix Luc-Screen and Galacto-Star Kits (Life Technologies) and quantified with a Chameleon plate luminometer (Hidex Personal Life Science). Transfection efficiencies were normalized to the β-galactosidase activities.

Chromatin immunoprecipitation (ChIP)

ChIP assays were carried out according to a protocol from the Furlong lab (Sandmann et al., 2006). Briefly, about one gram of synchronized embryos were collected, fixed and sonicated with a Bioruptor sonicator (Diagenode) to generate DNA fragments of ~500 bp in length. The immunoprecipitation were performed with anti-Brk serum (2 μl) or normal rabbit IgG (20 μg) and the subsequent steps were carried out as previously described (Fang et al., 2006). Primer pairs used in ChIP assays were 5′-accttctggctttggagcag-3′ and 5′-tgggctcctcataaactggc-3′ for CDS, 5′-tcaatcagacgtcagaggtaccg-3′ and 5′-ctgatggaagaaccgtgttgg-3′ for IntE^{Brk}.

In situ hybridization

In situ hybridizations for *nkd* in imaginal discs were performed as previously described (Chang et al., 2008a). For quantifying the *in situ* signals, images were processed in Adobe Photoshop, converted to gray scale and inverted (supplementary material Fig. S3). The mean gray values were measured by ImageJ (NIH, v1.46). Three nonoverlapping areas in the *nkd* expression domain (near D/V boundary) were sampled from both anterior or posterior compartments and, for each individual disc, the mean

gray values were measured and averaged, and the mean background value was subtracted from the average. Statistical analysis of the results was performed using ANOVA followed by post-hoc Tukey's test for comparison between groups. For fluorescence *in situ* hybridization (FISH), an *nkd* probe of the same sequence was labeled with biotin. After hybridization, TSA amplification (PerkinElmer) was applied and visualized by TRITC-strepavidin (1:300, Jackson Immunochemicals) and anti-GFP antibody (Roche) staining.

RESULTS

Brk interacts directly with an intronic region of *nkd*

We have previously shown that C-terminal Binding Protein (CtBP) directly represses *nkd*, a direct target of the Wg signaling pathway, via an intronic region of *nkd* (Fang et al., 2006). In addition, the physical binding of CtBP to the *nkd* locus is independent of TCF (Fang et al., 2006). However, CtBP functions as a transcriptional co-repressor and is not likely to bind to DNA directly (for a review, see Chinnadurai, 2002). In exploring the potential transcription factor that would recruit CtBP to DNA, two pieces of data drew our attention to Brk, a CtBP-binding repressor in Dpp signaling (Hasson et al., 2001; Zhang et al., 2001). By RNAi-mediated gene knockdown in *Drosophila* Kc167 (Kc) cells, we found that Brk repressed *nkd* expression in parallel with Gro (Fig. 1A), consistent with the synergistic repression of *nkd* by CtBP and Gro (Fang et al., 2006). We took advantage of the aligned genome sequences from 12 fly species (Stark et al., 2007) and identified a putative Brk recognition site (Sivasankaran et al., 2000; Rushlow et al., 2001; Zhang et al., 2001) within a completely conserved 66-bp sequence in the first intron of *nkd* (Fig. 1B; supplementary material Fig. S1). In addition to the presumptive Brk site, we also noticed two perfect neighboring TCF sites (Fig. 1B) (Chang et al., 2008b). Interestingly,

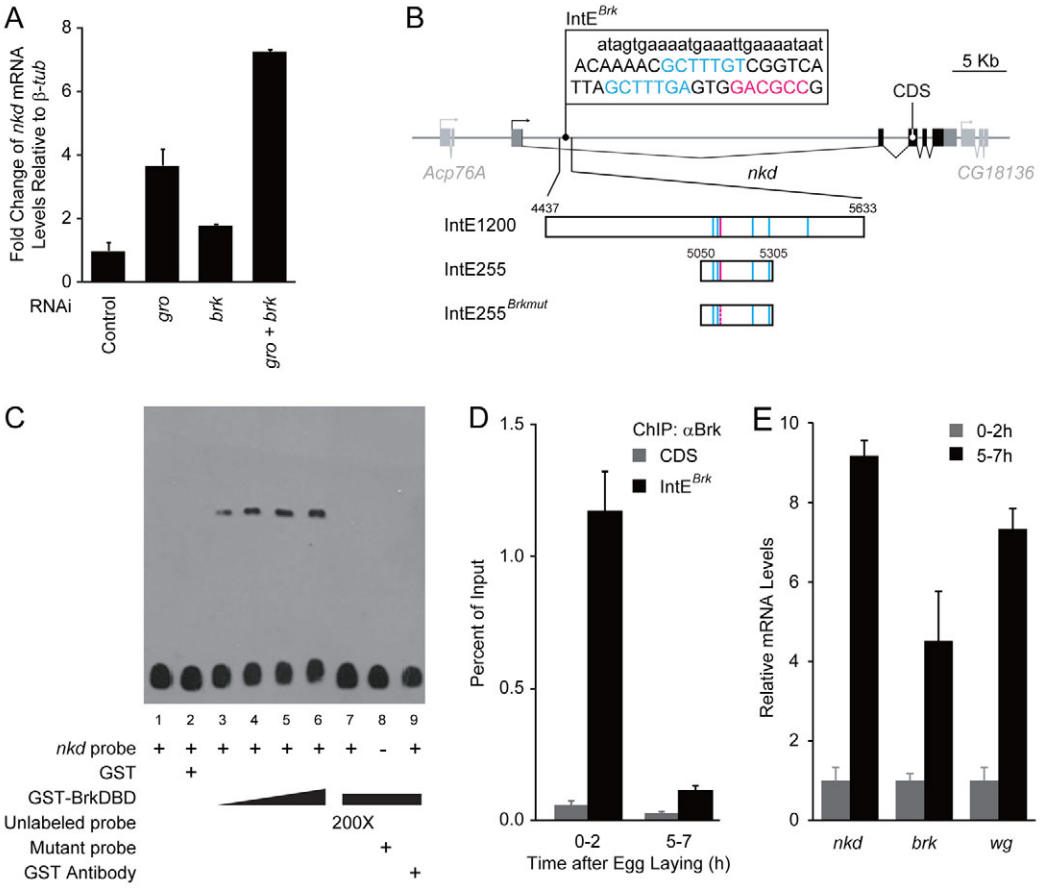

Fig. 1. Brk represses *nkd* and directly interacts with its intronic region *in vitro* and *in vivo*. (**A**) *Drosophila* Kc cells were treated with dsRNA(s) as indicated, and *nkd* mRNA levels were normalized by *β-tubulin56D* (*β-tub*) expression. Note that the double RNAi treatment against *brk* and *gro* induces higher *nkd* expression than any of the single RNAi treatments, indicating a synergetic repression of *nkd* by Brk and Gro. (**B**) Schematic of the *nkd* locus showing the location and sequence of a conserved 66-bp sequence (IntE^{Brk}) containing a presumptive a Brk site (pink) and two TCF sites (blue). The capital letters indicate the probe sequence in the EMSA assay shown in C. Regions for the ChIP analysis shown in D, IntE^{Brk} and CDS, are indicated. Also shown are sequence regions (IntE1200, IntE255 and IntE255^{Brkmut}) used in the reporter assays in Fig. 2, with bars standing for the predicted Brk site (pink) and TCF sites (blue) or a pink dashed bar for mutated Brk site. (**C**) Brk interacts with IntE^{Brk} *in vitro*. EMSA shows that a recombinant GST-BrkDBD fusion protein causes a dose-dependent shift of the probe (see B) (lanes 3-6), which is abolished by 200× excess unlabeled probe (lane 7), a mutant probe (lane 8) or anti-GST antibody (lane 9). (**D**) Brk occupies IntE^{Brk} *in vivo*, but only when Wg signaling is low. ChIP analysis using an anti-Brk antibody in fly embryos at 0-2 hours (when Wg signaling is low) and 5-7 hours AEL (when Wg is expressed) in DNA regions as indicated. DNA from ChIP was quantified by qPCR as described in the Materials and methods section. (**E**) Normalized mRNA levels of *nkd*, *brk* and *wg* relative to *β-tub* in the same embryos as in D. (A,E) mRNA levels were measured by RT-qPCR as described in the Materials and methods section. Data in A and D-E are representative results showing the averages from duplicate or triplicate sample sets, with error bars representing s.e.m. All experiments were carried out at least three times with similar results.

this 66-bp DNA region (referred to as IntE^{Brk}) falls into a region that was previously termed IntE and has been carefully characterized as one of the major WREs directing *nkd* expression in response to Wg signaling (Fang et al., 2006; Chang et al., 2008a).

To test whether Brk interacts directly with IntE^{Brk}, we performed an electrophoretic mobility shift assay (EMSA) using a recombined GST protein fused to the DNA-binding domain of Brk (GST-BrkDBD) (Jaźwińska et al., 1999; Saller and Bienz, 2001; Cordier et al., 2006). GST-BrkDBD caused a clear shift of a 40-bp IntE^{Brk} probe (Fig. 1B,C) in a dose-dependent manner, indicating a direct interaction between Brk and IntE^{Brk}. The interaction appeared to be specific: either an excessive amount of non-labeled probe or the addition of anti-GST antibody readily abolished the GST-BrkDBD-induced probe shift (Fig. 1C). Furthermore, we did not detect such a shift with a mutant probe in which three bases in the presumptive Brk site were substituted (Fig. 1C). Therefore, Brk is likely to interact with IntE^{Brk} via the Brk site that we have identified.

We next investigated whether Brk interacts with IntE^{Brk} *in vivo* and, if yes, whether such binding has any connection with Wg signaling? Therefore, we performed chromatin immunoprecipitation (ChIP) analysis on fly embryos. *wg* is initially expressed in embryos just prior to gastrulation, ~3 hours after egg laying (AEL), and functions as one of the major factors directing the patterning processes in fly segmentation (Bejsovec and Martinez Arias, 1991; Dougan and DiNardo, 1992). Accordingly, as a negative-feedback regulator of Wg signaling, *nkd* transcript was absent 0-2 hours AEL and reached its highest level 4-8 hours AEL in embryos (Zeng et al., 2000). We therefore made extracts from 0-2 hours and 5-7 hours AEL embryos to test the binding of Brk to IntE^{Brk}. Our data show that the physical occupation of Brk on this region was significant in 0-2 hours AEL embryos (Fig. 1D). In the 5-7 hours AEL embryos, however, the occupation of *nkd* by Brk was dramatically lower despite *brk* being expressed at a much higher level than in earlier embryos (Fig. 1D,E). These results indicate that Brk binds to *nkd in vivo* and that the physical occupation of *nkd* by Brk is inversely correlated with the level of Wg signaling.

Brk represses Arm-dependent activation of *nkd* intronic WRE in Kc cells

We have shown that Brk represses the Wg target *nkd* in Kc cells (Fig. 1A). To examine further whether Brk also influences Arm-dependent *nkd* activation, we carried out reporter assays in Kc cells using various fragments of the *nkd* intronic WRE (IntE), including IntE^{Brk}. As previously reported (Fang et al., 2006; Li et al., 2007; Chang et al., 2008a; Parker et al., 2008), IntE reporters are highly activated by a constitutively active form of Arm (Arm*) (Freeman and Bienz, 2001) in Kc cells. We observed that a 1.2-kb IntE reporter (IntE1200, Fig. 1B) ~4.5 kb downstream of the *nkd* transcription start site was activated ~100-fold following a moderate dose of transfected Arm* (Fig. 2A). Following co-transfection with a Brk expression vector, Arm-dependent activation of IntE1200 was inhibited by Brk in a dose-dependent fashion (Fig. 2A,E). Consistent with this observation, RNAi-mediated *brk* knockdown in Kc cells significantly increased the Arm*-dependent activation of IntE1200 (Fig. 2B,F). Similar results have been observed in a shorter, 255-bp version of IntE (IntE255; Fig. 1B; Fig. 2C,D) (Chang et al., 2008a). To test whether the Brk site in IntE255 is responsible for the inhibitory effect of Brk, we constructed a mutant reporter in a similar manner to the mutant probe used in the EMSA (IntE255^{Brkmut}; Fig. 1B). Although it still responded to Arm* stimulation, IntE255^{Brkmut} was no longer affected by the Brk protein (Fig. 2C,D). Consistent with our ChIP analysis in the embryos, these results indicate that Brk directly represses the intronic WRE activity upon Wg activation. The repressive role that we observed for Brk in these experiments cannot be explained by the interaction between Mad and TCF, as suggested by previous studies (Zeng et al., 2008; Eivers et al., 2011), because excess Brk did not affect the Arm-dependent activation of dTF12 (DasGupta et al., 2005), a Wg reporter composed of multimerized optimal TCF sites (supplementary material Fig. S2).

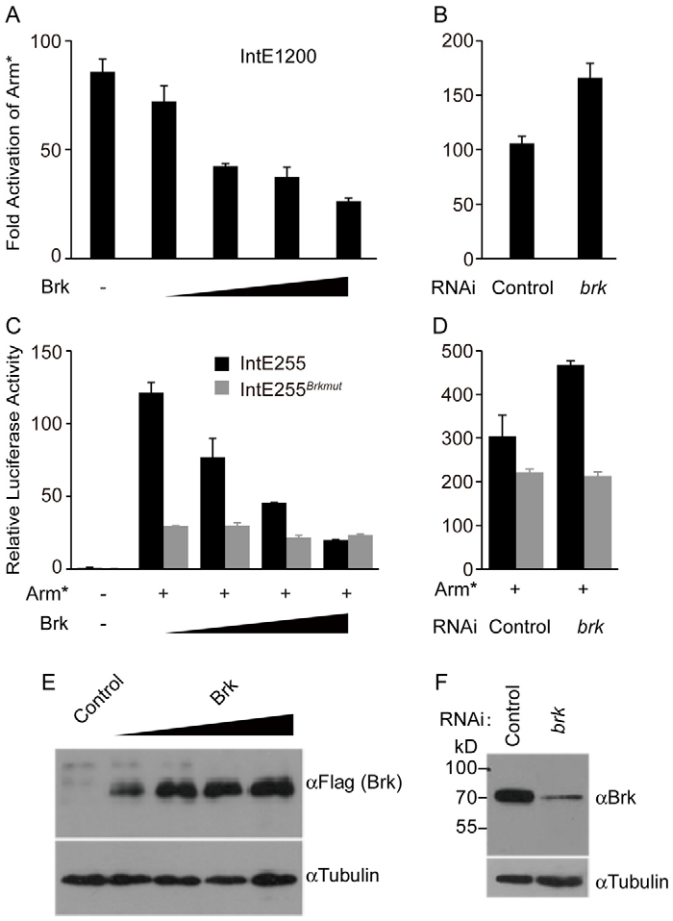

Fig. 2. Brk represses Arm-dependent activation of the intronic WRE in *nkd*. (**A-D**) Reporter assays in *Drosophila* Kc cells using the intronic regions IntE1200 (A,B) and IntE255 (C,D), as illustrated in Fig. 1B. A mutant version of the reporter for the Brk site (IntE255^{Brkmut}) is also used in C and D. Transfection of a moderate dose of constitutively active Arm* (10 ng/well) results in ~100-fold activation of both IntE1200 (A) and IntE255 (black columns in C). Co-transfection of a Flag-tagged Brk expression vector (10 ng, 20 ng, 40 ng and 80 ng per well) dose-dependently inhibits Arm*-dependent activation. Conversely, RNAi against *brk* results in enhanced Arm* activation of both reporters (B, black columns in D). Arm* readily activates IntE255^{Brkmut}, which is no longer affected by altered Brk expression (gray columns in C,D). Data are averages of duplicate or triplicate experiments, with error bars representing s.e.m. (**E**,**F**) Western blot analysis to confirm the expression levels of Brk in these experiments.

Brk represses *nkd* in fly wings

We have so far shown that Brk directly represses *nkd in vitro*. An obvious question is whether Brk also represses *nkd in vivo*. We made use of a *lacZ* reporter that is driven by a combination of WREs in the regulatory sequences in the *nkd* locus (*Nkd-lacZ*)

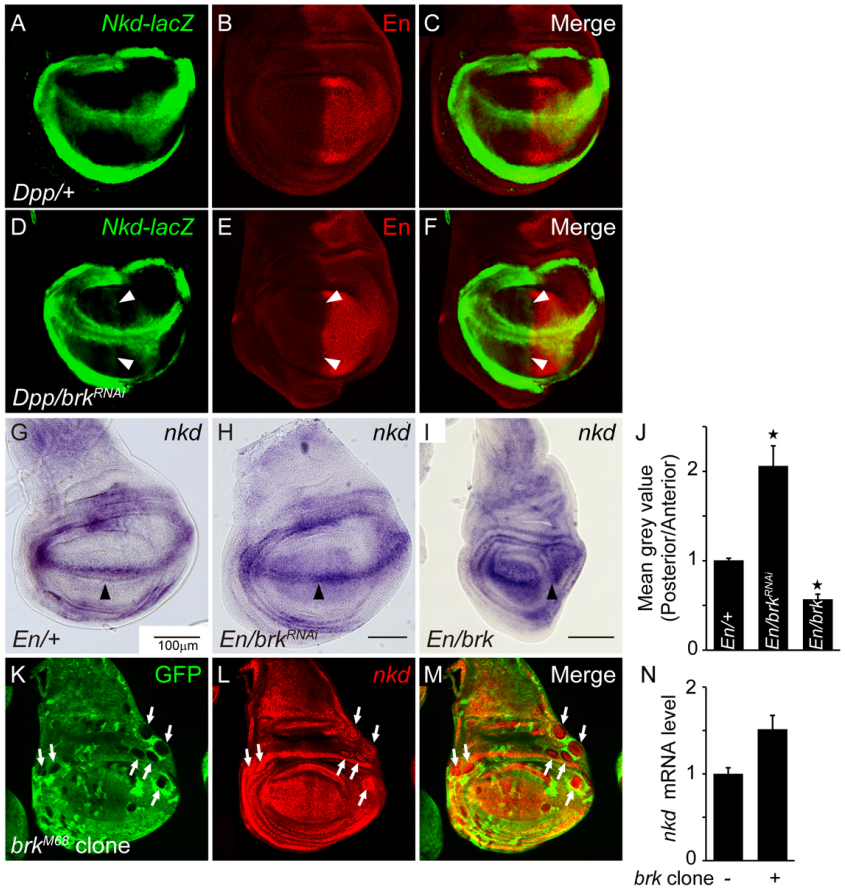

Fig. 3. Brk represses *nkd* expression in the wing imaginal discs. All images are taken from the third-instar wing discs and placed anterior to the left and dorsal up. (**A-F**) *Nkd-lacZ* reporter expressions (green) in flies with genotype P[*Dpp-Gal4*]/+ (A-C) and P[*Dpp-Gal4*]/[brk^{RNAi}] (D-F). Engrailed stainings (En, red) are used to indicate the A/P boundary. Note that the knockdown of *brk* causes the additional *lacZ* signal (white arrowheads) along A/P boundary where *Dpp-Gal4* activates. (**G-I**) *In situ* hybridization of *nkd* in wing discs with *En-Gal4* only (G, *En*/+), *En-Gal4* driven brk^{RNAi} (H, *En*/brk^{RNAi}) and *En-Gal4* driven *UAS-brk* (I, *En/brk*), as detailed in the Materials and methods section. A/P borders are marked by black arrowheads. Note that *nkd* is evenly expressed anteriorly and posteriorly in *En-Gal4*/+ wing disc (G), but is higher in posterior compartment of the *En*/brk^{RNAi} wing disc (H) and is lower posteriorly in *En/brk* ones. Note also the posterior compartments are enlarged in *En*/brk^{RNAi} and smaller in *En/brk* discs, presumably due to the effects on growth of the altered Dpp signaling. For *brk* RNAi, two independent *brk* RNAi lines, VDRC#GD2919 (shown in H) and VDRC#KK101887 (not shown), have been used and resulted in similar results. Scale bars: 100 μm. (**J**) Quantified expression levels of *nkd* in G-I. Data represent the average posterior to anterior ratios of mean gray values in the *nkd* expression domain, in flies bearing genotype of *En*/+ (n=14), *En*/brk^{RNAi} (n=5) and *En/brk* (n=11), with error bars standing for s.e.m. Stars indicate P<0.001 compared with *En*/+ group, as judged by one-way ANOVA followed by post-hoc Tukey's test for comparisons between the groups. (**K-M**) brk^{M68}clones were heat-shock induced in flies with a genotype of *yw* brk^{M68} *hsp70-flp FRT19A/yw hsp70-flp hsp70-GFP FRT19A*. FISH detection of *nkd* in brk^{M68} clones shows that the loss of *brk* results in dramatically increased *nkd* transcript levels, as marked by lack of GFP (arrows). (**N**) RT-qPCR analysis of *nkd* expression in third instar wing discs with or without clone induction, indicating a higher *nkd* expression when *brk* clones are induced. Error bars represent s.e.m.

(Chang et al., 2008a). When we knocked down *brk* using a *brk* RNAi line (*UAS-*brk^{RNAi}) driven by *Dpp-Gal4*, we detected an ectopic *lacZ* expression along the A/P boundary, as indicated by Engrailed expression (Fig. 3D-F), compared with control wing discs (Fig. 3A-C), suggesting that Brk represses *nkd* expression in wing discs. Consistent with this observation, by *in situ* hybridization we detected enhanced *nkd* transcript levels in the posterior half of the wing discs when brk^{RNAi} was driven by *Engrailed-Gal4* (*En-Gal4*) (Fig. 3G,H). Conversely, *En-Gal4*-driven *brk* overexpression caused reduced *nkd* transcription (Fig. 3I). These changes of *nkd* expression are significant when mean gray values are compared and judged by statistical analysis (Fig. 3J; supplementary material Fig. S3).

To examine this effect in a more rigorous way, we generated mitotic clones of a null allele of *brk*, brk^{M68} (Jaźwińska et al., 1999), and examined *nkd* transcripts in wing discs by fluorescence *in situ* hybridization (FISH). As expected, *nkd* FISH signals were dramatically increased in the *brk* clones (Fig. 3K-M). We noticed that *nkd* upregulations were more pronounced in *brk* clones positioned at A/P extremes, consistent with published studies that *brk* is expressed at higher levels in this region (Campbell and Tomlinson, 1999; Jaźwińska et al., 1999; Minami et al., 1999). In addition, we have used RT-qPCR analysis to confirm the increase of *nkd* transcripts in wing discs that underwent *brk* clones induction (Fig. 3N). Taken together, these data indicate that Brk represses *nkd* in wing discs.

Brk enhances Wg signaling in fly wings through the repression of *nkd*

To assess the role of *brk* in Wg signaling *in vivo*, we examined Wg targets, such as *Dll* and *senseless* (*sens*), in the wing imaginal disc.

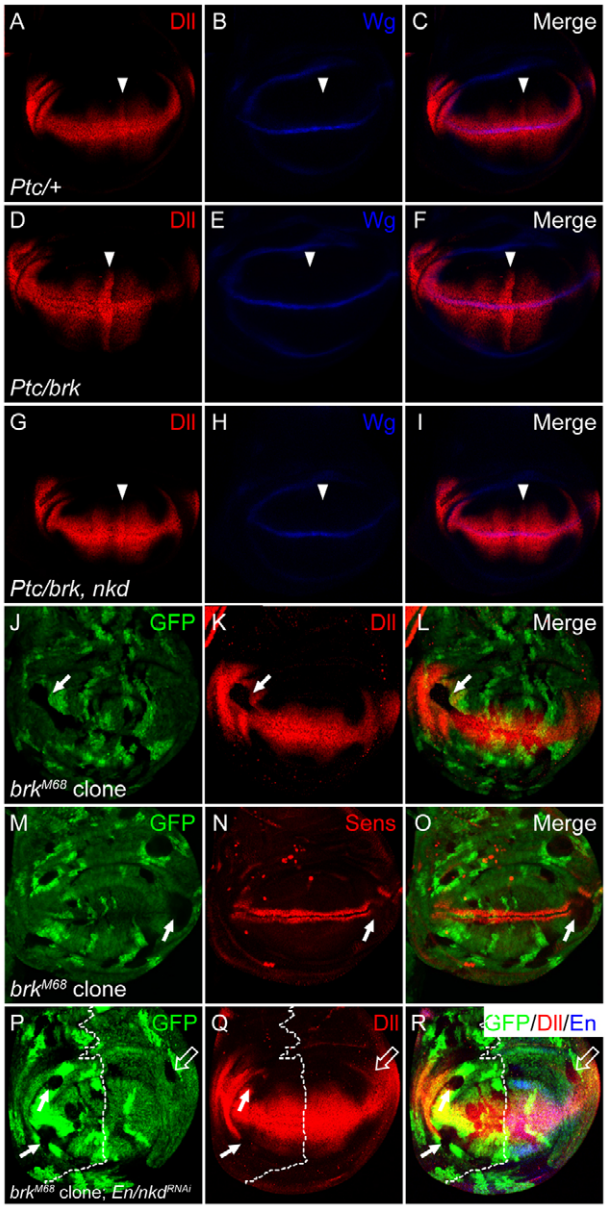

Fig. 4. *brk* is required for Wg target gene expression in wing imaginal discs. (**A-I**) Antibody staining in late third instar wing discs for Dll (red) and Wg (blue) in flies with genotypes of P[*Ptc-Gal4*]/+ (A-C, *Ptc*/+), P[*UAS-brk*]/P[*Ptc-Gal4*] (D-F, *Ptc/brk*) and P[*UAS-brk*], P[*UAS-nkd*]/P[*Ptc-Gal4*] (G-I, *Ptc/brk, nkd*). The A/P boundaries are indicated by downward arrowheads. Note that ectopic *brk* driven by *Ptc-Gal4* caused a marked expansion of Dll along the A/P border (D), compared with *Ptc-Gal4*/+ disc (A). Such an increase of Dll expression no longer exists in the wing disc co-expressing *brk* and *nkd* (G). No apparent alteration of Wg expression is observed in these discs (B,E,H). (**J-O**) Antibody staining of Dll (J-L) and Sens (M-O) in brk^{M68} clones, which were produced as in Fig. 3K and marked by the lack of GFP. Note the clone across hinge and wing pouch areas, indicated by arrows, in J-L. Dll is completely disrupted in hinge area but remains unaffected within wing pouch. A clone in M-O also shows reduced Sens expression (arrows). (**P-R**) brk^{M68} clones are generated in the genetic background of *nkd* RNAi driven by *En-Gal4* driver. Note that Dll (red) expression is disrupted in *brk* clones (arrows) in anterior compartment but is normal in a *brk* clone (unfilled arrow) in the posterior half where *nkd* expression is knocked down. A/P border is marked by the white dotted lines according to En expression (R).

Ectopic *brk* driven by *Patched-Gal4* (*Ptc-Gal4*), which is activated along the A/P compartment boundary, caused an expansion of Dll expression (Fig. 4A-F), whereas Wg expression was not affected. Based on our conclusion from Fig. 3 that Brk represses *nkd*, the increased Dll expression could be due to the lowered expression of Nkd, the negative regulator of Wg signaling. If so, then ectopic *nkd* should be able to abolish Dll expansions caused by the over production of *brk*. Indeed, we found that co-expression of *nkd* with *brk* gave rise to similar Dll patterns to those seen in control discs (Fig. 4G-I). These observations are consistent with the notion that *brk* enhances Wg signaling.

To look into the possible effects of endogenous *brk* on Wg signaling, we examined Dll and Sens expressions in the brk^{M68} clones. Dll expression in these clones was not always the same. We did not observe a detectable change of Dll expression in *brk* clones positioned within wing pouch areas. However, in clones away from A/P boundary, both anteriorly and posteriorly in hinge areas, we saw dramatic Dll reductions (supplementary material Fig. S4). Fig. 4J-L shows a typical *brk* clone across the hinge and wing pouch, in which Dll was completely absent in the hinge region but was unaffected in the wing pouch area. Such a positional effect is consistent with the observation of increased *nkd* expression in *brk* clones (Fig. 3K-M) and might reflect a dosage dependence of *brk*. The hinge expression of Dll depends on canonical Wg signaling, as Dll was significantly reduced in *pygo* clones in this area (supplementary material Fig. S5) (Parker et al., 2002). Wg was not affected in *brk* clones (supplementary material Fig. S6), indicating that the reduction of Dll expression was not due to a direct change in Wg expression. Similar results were observed for Sens, another Wg target in wing discs (Fig. 4M-O). Again, if it stands true that the reduced Dll level in *brk* clones is due to de-repressed *nkd* expression, it should be reversed in a loss-of-*nkd* background. To test this, we used a UAS-RNAi allele ($UAS\text{-}nkd^{RNAi}$) generated according to *nkd* sequence. As shown in supplementary material Fig. S7, *En-Gal4*-driven $UAS\text{-}nkd^{RNAi}$ dramatically knocked down *nkd* levels in the posterior compartment. Therefore, we examined Dll expression in *brk* clones in this *nkd* RNAi background. We did observe that Dll expression was lost in anterior *brk* clones but not in posterior ones in the hinge (Fig. 4P-R), indicating a need for *nkd* in the reduction of Wg signaling in *brk* clones. Together, these results demonstrate that *brk* is required for Wg signaling in hinge area of wing discs.

The data described thus far indicate that Brk represses *nkd* and is required for Wg target gene expression in the wing disc. Is *brk* also required for adult wing structures? It is well documented that the wing margin is defined and patterned from a stripe of cells expressing *wg* during the third instar larvae (Phillips and Whittle, 1993; Couso et al., 1994). Loss of Wg signaling leads to defects of the adult wing margin, characterized by loss of bristles and/or notches in the wing. Conversely, elevated Wg signaling typically causes extra bristles.

Consistent with a role of *brk* in wing margin formation, studies from independent laboratories have shown that loss of *brk* results in notched wing in addition to wing outgrowths (Campbell and Tomlinson, 1999; Jaźwińska et al., 1999). To examine this in more detail, we analyzed wing phenotypes in brk^{M68} clones in a more quantitative way. In flies potentially bearing *brk* clones, we found that 19% of the flies gave rise to notches in the wing, a phenotype indicative of a loss of Wg signaling (Fig. 5C; n=163). In addition, we saw many swirled hairs in areas close to the wing notches (Fig. 5D), which are consistent with the previous finding that a timed over production of *nkd* gives rise to planar cell polarity

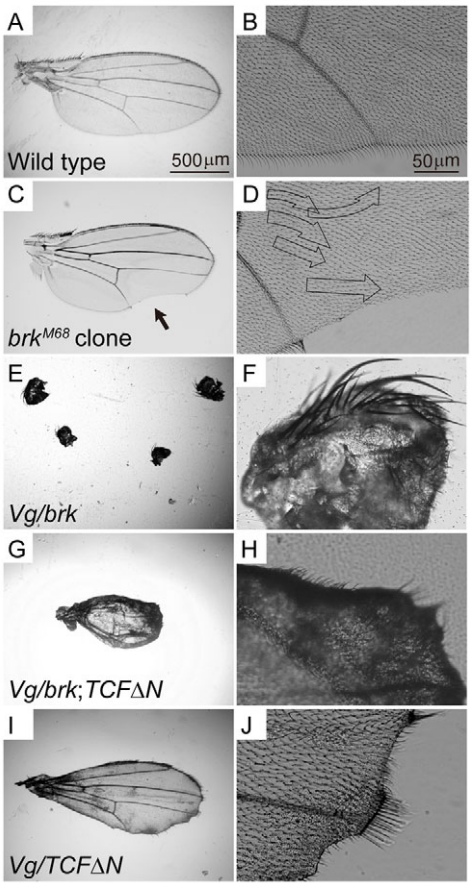

Fig. 5. Loss and gain of *brk* phenocopies the loss and gain of Wg signaling in adult wings. Images of adult wings from wild-type flies (A,B), flies bearing the brk^{M68} clones as in Fig. 3J-L (C,D) and flies with genotypes of P[*Vg-Gal4*]/P[*UAS-brk*] (E,F, *Vg/brk*), P[*Vg-Gal4*]/P[*UAS-brk*]; P[*UAS-TCFΔN*]/+ (G,H, *Vg/brk*; *TCFΔN*) and P[*Vg-Gal4*]/+; P[*UAS-TCFΔN*]/+ (I,J, *Vg/TCFΔN*). Right panels are enlarged views from the corresponding left ones. (**A**,**B**) Morphology of wild-type wing displays an intact wing margin. (**C**,**D**) Adult wing bearing *brk* clones presents a notched phenotype (arrow), often seen in flies with reduced Wg signaling, at a penetrance of 19% (*n*=163), but with much less frequent (5%, *n*=163) outgrowth events. Defects in bristle arrangement are also observed on the wing surface as marked by unfilled arrows, similar to planer cell polarity deficits reported in wings overexpressing *nkd* (Rousset et al., 2001). (**E**,**F**) Ectopic expression of *Vg-Gal4*-driven *brk* results in a much smaller wing, as previously reported (Martín et al., 2004), but also stout bristles indicative of a gain in Wg signaling. (**G**,**H**) Co-expression of *TCFΔN*, a known inhibitor of Wg signaling (**I**,**J**) (van de Wetering et al., 1997), suppresses phenotypes caused by ectopic *brk* in E,F.

(PCP) phenotypes (Rousset et al., 2001). By contrast, we only occasionally saw (5%, *n*=163) wing outgrowths in these flies. These results may indicate that aside from a repressive role of Brk in Dpp signaling, Brk might play an essential role in Wg signaling. In further support of this notion, in wings with ectopic *brk* driven by *Vestigial-Gal4* (*Vg-Gal4*), we often observed stout bristles indicative of a gain of Wg signaling (Fig. 5E,F) (Couso et al., 1994; Zhang and Carthew, 1998; Zeng et al., 2008), although the wings were much smaller compared with wild-type flies, as previously reported (Martín et al., 2004). Furthermore, co-expression of *TCFΔN*, which inhibits Wg signaling (van de Wetering et al., 1997) as evidenced by causing notches (Fig. 5I,J),

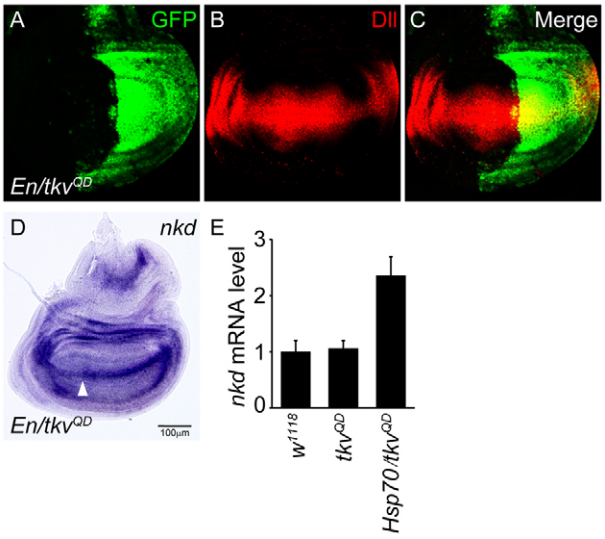

Fig. 6. Dpp signaling promotes *nkd* transcription and inhibits Dll expression. (**A-C**) A wing disc of P[*UAS-GFP*]; P[*UAS-tkv^{QD}*]/P[*En-Gal4*] (*En/tkv^{QD}*) stained with Dll (B, red). In this wing disc, with ectopic Dpp signaling due to *En-Gal4*-driven tkv^{QD}, Dll is apparently expressed in a narrower pattern in the posterior half than in the anterior region (B), indicating a significant decrease in Dll expression. (**D**) *In situ* hybridization of *nkd* in *En/tkv^{QD}* wing discs shows an enhanced *nkd* signal in the posterior half. A/P border is indicated by an upward arrowhead. Note the apparently wider posterior half due to gain of Dpp signaling, consistent with previous studies (Schwank et al., 2008). Scale bar: 100 μm. (**E**) qPCR quantification of *nkd* in adult flies of genotypes w^{1118}, P[*UAS-tkv^{QD}*] (*tkv^{QD}*) and P[*Hsp70-Gal4*] (*Hsp70/tkv^{QD}*, subjected to heat shock as detailed in the Materials and methods section), normalized to *β-tub*. Note the marked increase of *nkd* in the *Hsp70/tkv^{QD}* flies. Data are the averages of two groups of flies, and the errors bars represent s.e.m. The experiment was carried out twice with similar results.

suppressed these stout bristles (Fig. 5G,H). We interpreted these results as evidence that Brk antagonizes Dpp signaling and promotes Wg signaling at the same time. From the experiments inducing the loss or gain of *brk* in fly wings, we have found phenotypes resembling those observed in the loss or gain of Wg signaling, respectively, which might have been overlooked in previous studies.

The Dpp pathway is also involved in the regulation of Wg targets

As mentioned earlier, *brk* is directly repressed by Dpp signaling (reviewed by Affolter and Basler, 2007). According to our model, increasing Dpp signaling should also increase *nkd* expression and inhibit Wg signaling in the wing. Indeed, Tkv^{QD}, a constitutively active form of the Dpp receptor, increased *nkd* expression in the wing disc and globally in adult flies (Fig. 6D,E). In wing discs, Dll is considered to be a long-range target of Wg (Zecca et al., 1996; Neumann and Cohen, 1997) and is normally expressed at a comparatively low level close to the A/P boundary, resulting in two expanded domains with one being slightly wider in the posterior region (Fig. 3A). When *tkv^{QD}* was overexpressed in the posterior half by *En-Gal4*, Dll was expressed in a domain that was apparently narrower posteriorly than anteriorly (Fig. 6A-C), indicating a significant decrease in Dll expression. These results clearly show that Dpp signaling promotes *nkd* expression and suppresses Wg signaling in wing discs.

DISCUSSION

In this study, we have shown that Brk directly represses *nkd* expression *in vitro* and *in vivo*. The direct repression of *nkd* by Brk is underscored by three of our observations. First, we have identified a Brk site in the intronic region of *nkd*, which Brk physically occupies *in vitro* (Fig. 1B,C). Second, ChIP analysis shows that Brk binds a DNA region near this Brk site in embryos in a manner inversely related to Wg activity (Fig. 1D,E). Third, our reporter analysis in Kc cells indicates that Brk represses Arm-dependent activation of an intronic WRE containing this Brk site, but only when the Brk site is intact (Fig. 2). In addition, our genetic analyses have shown that the repression of *nkd* by Brk is functionally significant. In the developing wing, we found that the loss of *brk* de-represses *nkd* (Fig. 3) and downregulates Wg target proteins, such as Dll and Sens (Fig. 4). Conversely, ectopic *brk* inhibits *nkd* expression (Fig. 3) and markedly enhances Dll expression (Fig. 4). Furthermore, removal of *nkd* prevents the loss of Dll in *brk* clones whereas co-expression of *nkd* abolishes the expanded Dll caused by ectopic *brk* (Fig. 4). In adult wing, the loss and gain of *brk* phenotypically resembles the loss and gain of Wg signaling, respectively (Fig. 5). Consistent with a repressive role of Dpp cascade on *brk*, we found that ectopic Dpp signaling enhances *nkd* and inhibits Wg signaling (Fig. 6). These results support a model in which Dpp signaling increases the expression of Nkd, a Wg inhibitor, by the downregulation of Brk, and thereby inhibits the Wg outputs. In another words, *nkd* might fall into a class of Dpp targets, which are de-repressed upon the activation of Dpp signaling. We have thus uncovered a previously unsuspected molecular mechanism underlying the interaction between Wg and Dpp signaling pathways in *Drosophila* wing development.

Until recently, little has been known about the cross-interaction between Wg and Dpp signaling in *Drosophila* wings, in spite of the fact that the fly wing has served as an excellent model system for the dissection of the molecular basis of these signaling transduction pathways. This is in contrast to *Drosophila* leg imaginal discs, in which mutual repression between Wg and Dpp signaling has long been suspected. However, several studies have indicated that manipulation of Dpp signaling levels in the wing sometimes leads to phenotypes resembling those caused by loss or gain of Wg activity. Notably, ectopic Dpp signaling increases notches in the wing (Marquez et al., 2001; Bennett and Alphey, 2002; Zeng et al., 2008), which is characteristic of reduced Wg signaling (Couso et al., 1994). However, the underlying mechanism for this effect of Dpp is not clear. Recently, independent research groups have suggested that Mad, the key effector of Dpp signaling, might play a role in the regulation of Wg target gene expression in fly wings (Zeng et al., 2008; Eivers et al., 2011). The molecular basis for their findings has mainly been the physical interaction between Mad and TCF, similar to the findings in mammals, in which several Smad proteins interact with members of the lymphoid enhancer binding factor 1/TCF family of DNA-binding HMG box transcription factors (Labbé et al., 2000; Hussein et al., 2003; Labbé et al., 2007; Minoo and Li, 2010). It remains to be determined whether the role of Mad is direct or indirect because the reporter assays in these studies were performed with TOPFlash (Korinek et al., 1997) or similar constructs in mammalian cell culture, which might not always accurately represent the complicated situation of the *in vivo* regulation of Wg target genes (Chang et al., 2008b). Furthermore, manipulation of Mad expression in wing discs influences Dll expression in different directions (Zeng et al., 2008; Eivers et al., 2011). Although these intriguing discrepancies can be explained by the physical interaction between Mad and TCF, our model offers an alternative interpretation based on the negative regulation of *nkd* by Brk, which might suggest an indirect role of Mad in Wg signaling. For example, our model could provide an explanation for the previous finding that ectopic Dpp signaling, caused by Mad, Medea, Tkv^{QD}, etc., results in notched wings (Zeng et al., 2008).

The role of Brk in Wg signaling has been previously documented in *Drosophila*. It has been suggested that *brk* is able to antagonize Wg signaling based on the activity of a midgut-specific Ubx reporter gene in which physical interactions among Brk, Teashirt and CtBP have been described (Saller et al., 2002). In leg discs, Wg signaling may directly repress Dpp morphogen expression via an Arm-TCF-Brk complex, offering a direct model for the cross-talk between Wg and Dpp (Theisen et al., 2007). However, our studies have indicated a positive role for Brk in Wg signaling through an indirect action. In addition to the repression of Dpp targets, the roles of Brk in Wg signaling described in these different models exemplify the pleiotropic actions of *brk* throughout development and might provide the molecular basis for tissue-specific consequences of developmental signaling pathways.

nkd was first identified as a *Drosophila* segment-polarity gene, mutation of which gives rise to major deficits in fly embryonic development (Jürgens et al., 1984). Its expression appears to be universally induced by Wg in fly embryos and larval imaginal discs (Zeng et al., 2000). It is interesting that although the loss of *nkd* in embryos has an effect similar to gain of *wg*, decreased *nkd* function in fly wings shows little impact (Zeng et al., 2000). However, none of the *nkd* alleles used in these studies has been well characterized at the molecular level (Zeng et al., 2000). Given the complexity of *nkd* transcriptional regulation (Chang et al., 2008a), it could be that these mutant forms of *nkd* still possess residual function in the wing. Alternately, overexpression of *nkd* blocks ectopic Wg signaling in the eyes and generates PCP phenotypes in the wing through a direct interaction with Dsh (Rousset et al., 2001). Consistent with these observations, we found that loss of *brk* can cause a dramatic increase of *nkd* expression in certain areas of the wing imaginal disc, leading to wing notches and PCP defects (Fig. 5D). Our findings suggest that *nkd* may indeed play roles, at a certain level, in both canonical and noncanonical Wg signaling in fly wings. However, a closer examination of *nkd* function in fly wings is needed.

In conclusion, we found that Brk influences Wg signaling by directly repressing *nkd* expression and could serve as a node for cross-talk between the Wg and Dpp signaling pathways. Wnt-BMP cross-interactions have been implicated in many developmental and disease processes (Itasaki and Hoppler, 2010). For example, a Wnt-BMP feedback circuit mechanism is important for inter-tissue signaling dynamics in tooth organogenesis in mouse (O'Connell et al., 2012). Our findings may therefore add new insights into cell differentiation and human cancer.

Acknowledgements

The authors thank Drs Ken Cadigan, Zhijun Shen and Haiyun Song for their critical reading and editorial help during the preparation of the manuscript; Drs Ken Cadigan, Hugo Bellen, Sean Carroll, Konrad Basler, Stuart Newfeld, Lei Xue, Helen Skaer for reagents; and Bloomington Stock Center, Vienna *Drosophila* RNAi Center and Developmental Studies Hybridoma Bank for flies and antibodies.

Funding

This work is supported by grants from the National Basic Research Program of China [2012CB517904] and the Natural Science Foundation of China [31070826 and 90608019] to M.F.

Competing interests statement
The authors declare no competing financial interests.

Supplementary material
Supplementary material available online at
http://dev.biologists.org/lookup/suppl/doi:10.1242/dev.082578/-/DC1

References

Affolter, M. and Basler, K. (2007). The Decapentaplegic morphogen gradient: from pattern formation to growth regulation. *Nat. Rev. Genet.* **8**, 663-674.
Affolter, M., Marty, T., Vigano, M. A. and Ja wi ska, A. (2001). Nuclear interpretation of Dpp signaling in Drosophila. *EMBO J.* **20**, 3298-3305.
Bejsovec, A. and Martinez Arias, A. (1991). Roles of wingless in patterning the larval epidermis of Drosophila. *Development* **113**, 471-485.
Bennett, D. and Alphey, L. (2002). PP1 binds Sara and negatively regulates Dpp signaling in Drosophila melanogaster. *Nat. Genet.* **31**, 419-423.
Brook, W. J. and Cohen, S. M. (1996). Antagonistic interactions between wingless and decapentaplegic responsible for dorsal-ventral pattern in the Drosophila Leg. *Science* **273**, 1373-1377.
Cadigan, K. M. (2002). Regulating morphogen gradients in the Drosophila wing. *Semin. Cell Dev. Biol.* **13**, 83-90.
Cadigan, K. M. (2012). TCFs and Wnt/ -catenin signaling: more than one way to throw the switch. *Curr. Top. Dev. Biol.* **98**, 1-34.
Campbell, G. and Tomlinson, A. (1999). Transducing the Dpp morphogen gradient in the wing of Drosophila: regulation of Dpp targets by brinker. *Cell* **96**, 553-562.
Chang, J. L., Chang, M. V., Barolo, S. and Cadigan, K. M. (2008a). Regulation of the feedback antagonist naked cuticle by Wingless signaling. *Dev. Biol.* **321**, 446-454.
Chang, M. V., Chang, J. L., Gangopadhyay, A., Shearer, A. and Cadigan, K. M. (2008b). Activation of wingless targets requires bipartite recognition of DNA by TCF. *Curr. Biol.* **18**, 1877-1881.
Chinnadurai, G. (2002). CtBP, an unconventional transcriptional corepressor in development and oncogenesis. *Mol. Cell* **9**, 213-224.
Cordier, F., Hartmann, B., Rogowski, M., Affolter, M. and Grzesiek, S. (2006). DNA recognition by the brinker repressor – an extreme case of coupling between binding and folding. *J. Mol. Biol.* **361**, 659-672.
Couso, J. P., Bishop, S. A. and Martinez Arias, A. (1994). The wingless signalling pathway and the patterning of the wing margin in Drosophila. *Development* **120**, 621-636.
DasGupta, R., Kaykas, A., Moon, R. T. and Perrimon, N. (2005). Functional genomic analysis of the Wnt-wingless signaling pathway. *Science* **308**, 826-833.
Dougan, S. and DiNardo, S. (1992). Drosophila wingless generates cell type diversity among engrailed expressing cells. *Nature* **360**, 347-350.
Eivers, E., Fuentealba, L. C., Sander, V., Clemens, J. C., Hartnett, L. and De Robertis, E. M. (2009). Mad is required for wingless signaling in wing development and segment patterning in Drosophila. *PLoS ONE* **4**, e6543.
Eivers, E., Demagny, H., Choi, R. H. and De Robertis, E. M. (2011). Phosphorylation of Mad controls competition between wingless and BMP signaling. *Sci. Signal.* **4**, ra68.
Estella, C., McKay, D. J. and Mann, R. S. (2008). Molecular integration of wingless, decapentaplegic, and autoregulatory inputs into Distalless during Drosophila leg development. *Dev. Cell* **14**, 86-96.
Fang, M., Li, J., Blauwkamp, T., Bhambhani, C., Campbell, N. and Cadigan, K. M. (2006). C-terminal-binding protein directly activates and represses Wnt transcriptional targets in Drosophila. *EMBO J.* **25**, 2735-2745.
Freeman, M. and Bienz, M. (2001). EGF receptor/Rolled MAP kinase signalling protects cells against activated Armadillo in the Drosophila eye. *EMBO Rep.* **2**, 157-162.
Gerlitz, O. and Basler, K. (2002). Wingful, an extracellular feedback inhibitor of Wingless. *Genes Dev.* **16**, 1055-1059.
Hasson, P., Müller, B., Basler, K. and Paroush, Z. (2001). Brinker requires two corepressors for maximal and versatile repression in Dpp signalling. *EMBO J.* **20**, 5725-5736.
Hussein, S. M., Duff, E. K. and Sirard, C. (2003). Smad4 and beta-catenin co-activators functionally interact with lymphoid-enhancing factor to regulate graded expression of Msx2. *J. Biol. Chem.* **278**, 48805-48814.
Itasaki, N. and Hoppler, S. (2010). Crosstalk between Wnt and bone morphogenic protein signaling: a turbulent relationship. *Dev. Dyn.* **239**, 16-33.
Jaźwińska, A., Kirov, N., Wieschaus, E., Roth, S. and Rushlow, C. (1999). The Drosophila gene brinker reveals a novel mechanism of Dpp target gene regulation. *Cell* **96**, 563-573.
Jiang, J. and Struhl, G. (1996). Complementary and mutually exclusive activities of decapentaplegic and wingless organize axial patterning during Drosophila leg development. *Cell* **86**, 401-409.
Jürgens, G., Wieschaus, E., Nüsslein-Volhard, C. and Kluding, H. (1984). Mutations affecting the pattern of the larval cuticle in Drosophila melanogaster. II. Zygotic loci on the third chromosome. *Roux's Arch. Dev. Biol.* **193**, 283-295.
Johnston, L. A. and Schubiger, G. (1996). Ectopic expression of wingless in imaginal discs interferes with decapentaplegic expression and alters cell determination. *Development* **122**, 3519-3529.
Korinek, V., Barker, N., Morin, P. J., van Wichen, D., de Weger, R., Kinzler, K. W., Vogelstein, B. and Clevers, H. (1997). Constitutive transcriptional activation by a beta-catenin-Tcf complex in APC-/- colon carcinoma. *Science* **275**, 1784-1787.
Labbé, E., Letamendia, A. and Attisano, L. (2000). Association of Smads with lymphoid enhancer binding factor 1/T cell-specific factor mediates cooperative signaling by the transforming growth factor-beta and wnt pathways. *Proc. Natl. Acad. Sci. USA* **97**, 8358-8363.
Labbé, E., Lock, L., Letamendia, A., Gorska, A. E., Gryfe, R., Gallinger, S., Moses, H. L. and Attisano, L. (2007). Transcriptional cooperation between the transforming growth factor-beta and Wnt pathways in mammary and intestinal tumorigenesis. *Cancer Res.* **67**, 75-84.
Li, J., Sutter, C., Parker, D. S., Blauwkamp, T., Fang, M. and Cadigan, K. M. (2007). CBP/p300 are bimodal regulators of Wnt signaling. *EMBO J.* **26**, 2284-2294.
Marquez, R. M., Singer, M. A., Takaesu, N. T., Waldrip, W. R., Kraytsberg, Y. and Newfeld, S. J. (2001). Transgenic analysis of the Smad family of TGF-beta signal transducers in Drosophila melanogaster suggests new roles and new interactions between family members. *Genetics* **157**, 1639-1648.
Martín, F. A., Pérez-Garijo, A., Moreno, E. and Morata, G. (2004). The brinker gradient controls wing growth in Drosophila. *Development* **131**, 4921-4930.
Minami, M., Kinoshita, N., Kamoshida, Y., Tanimoto, H. and Tabata, T. (1999). brinker is a target of Dpp in Drosophila that negatively regulates Dpp-dependent genes. *Nature* **398**, 242-246.
Minoo, P. and Li, C. (2010). Cross-talk between transforming growth factor-beta and Wingless/Int pathways in lung development and disease. *Int. J. Biochem. Cell Biol.* **42**, 809-812.
Morata, G. (2001). How Drosophila appendages develop. *Nat. Rev. Mol. Cell Biol.* **2**, 89-97.
Morimura, S., Maves, L., Chen, Y. and Hoffmann, F. M. (1996). decapentaplegic overexpression affects Drosophila wing and leg imaginal disc development and wingless expression. *Dev. Biol.* **177**, 136-151.
Müller, B., Hartmann, B., Pyrowolakis, G., Affolter, M. and Basler, K. (2003). Conversion of an extracellular Dpp/BMP morphogen gradient into an inverse transcriptional gradient. *Cell* **113**, 221-233.
Nellen, D., Burke, R., Struhl, G. and Basler, K. (1996). Direct and long-range action of a DPP morphogen gradient. *Cell* **85**, 357-368.
Neumann, C. J. and Cohen, S. M. (1997). Long-range action of Wingless organizes the dorsal-ventral axis of the Drosophila wing. *Development* **124**, 871-880.
Nolo, R., Abbott, L. A. and Bellen, H. J. (2000). Senseless, a Zn finger transcription factor, is necessary and sufficient for sensory organ development in Drosophila. *Cell* **102**, 349-362.
O'Connell, D. J., Ho, J. W., Mammoto, T., Turbe-Doan, A., O'Connell, J. T., Haseley, P. S., Koo, S., Kamiya, N., Ingber, D. E., Park, P. J. et al. (2012). A Wnt-bmp feedback circuit controls intertissue signaling dynamics in tooth organogenesis. *Sci. Signal.* **5**, ra4.
Panganiban, G., Sebring, A., Nagy, L. and Carroll, S. (1995). The development of crustacean limbs and the evolution of arthropods. *Science* **270**, 1363-1366.
Parker, D. S., Jemison, J. and Cadigan, K. M. (2002). Pygopus, a nuclear PHD-finger protein required for Wingless signaling in Drosophila. *Development* **129**, 2565-2576.
Parker, D. S., Ni, Y. Y., Chang, J. L., Li, J. and Cadigan, K. M. (2008). Wingless signaling induces widespread chromatin remodeling of target loci. *Mol. Cell. Biol.* **28**, 1815-1828.
Penton, A. and Hoffmann, F. M. (1996). Decapentaplegic restricts the domain of wingless during Drosophila limb patterning. *Nature* **382**, 162-164.
Phillips, R. G. and Whittle, J. R. (1993). wingless expression mediates determination of peripheral nervous system elements in late stages of Drosophila wing disc development. *Development* **118**, 427-438.
Rousset, R., Mack, J. A., Wharton, K. A., Jr, Axelrod, J. D., Cadigan, K. M., Fish, M. P., Nusse, R. and Scott, M. P. (2001). Naked cuticle targets dishevelled to antagonize Wnt signal transduction. *Genes Dev.* **15**, 658-671.
Rushlow, C., Colosimo, P. F., Lin, M. C., Xu, M. and Kirov, N. (2001). Transcriptional regulation of the Drosophila gene zen by competing Smad and Brinker inputs. *Genes Dev.* **15**, 340-351.
Saller, E. and Bienz, M. (2001). Direct competition between Brinker and Drosophila Mad in Dpp target gene transcription. *EMBO Rep.* **2**, 298-305.
Saller, E., Kelley, A. and Bienz, M. (2002). The transcriptional repressor Brinker antagonizes Wingless signaling. *Genes Dev.* **16**, 1828-1838.
Sandmann, T., Jakobsen, J. S. and Furlong, E. E. (2006). ChIP-on-chip protocol for genome-wide analysis of transcription factor binding in Drosophila melanogaster embryos. *Nat. Protoc.* **1**, 2839-2855.

Schwank, G., Restrepo, S. and Basler, K. (2008). Growth regulation by Dpp: an essential role for Brinker and a non-essential role for graded signaling levels. *Development* **135**, 4003-4013.
Sivasankaran, R., Vigano, M. A., Müller, B., Affolter, M. and Basler, K. (2000). Direct transcriptional control of the Dpp target omb by the DNA binding protein Brinker. *EMBO J.* **19**, 6162-6172.
Stark, A., Lin, M. F., Kheradpour, P., Pedersen, J. S., Parts, L., Carlson, J. W., Crosby, M. A., Rasmussen, M. D., Roy, S., Deoras, A. N. et al. (2007). Discovery of functional elements in 12 Drosophila genomes using evolutionary signatures. *Nature* **450**, 219-232.
Tabata, T. and Takei, Y. (2004). Morphogens, their identification and regulation. *Development* **131**, 703-712.
Theisen, H., Haerry, T. E., O'Connor, M. B. and Marsh, J. L. (1996). Developmental territories created by mutual antagonism between Wingless and Decapentaplegic. *Development* **122**, 3939-3948.
Theisen, H., Syed, A., Nguyen, B. T., Lukacsovich, T., Purcell, J., Srivastava, G. P., Iron, D., Gaudenz, K., Nie, Q., Wan, F. Y. et al. (2007). Wingless directly represses DPP morphogen expression via an armadillo/TCF/Brinker complex. *PLoS ONE* **2**, e142.
van de Wetering, M., Cavallo, R., Dooijes, D., van Beest, M., van Es, J., Loureiro, J., Ypma, A., Hursh, D., Jones, T., Bejsovec, A. et al. (1997). Armadillo coactivates transcription driven by the product of the Drosophila segment polarity gene dTCF. *Cell* **88**, 789-799.
Wisotzkey, R. G., Mehra, A., Sutherland, D. J., Dobens, L. L., Liu, X., Dohrmann, C., Attisano, L. and Raftery, L. A. (1998). Medea is a Drosophila Smad4 homolog that is differentially required to potentiate DPP responses. *Development* **125**, 1433-1445.
Worby, C. A., Simonson-Leff, N. and Dixon, J. E. (2001). RNA interference of gene expression (RNAi) in cultured Drosophila cells. *Sci. STKE* **2001**, pl1.
Zecca, M., Basler, K. and Struhl, G. (1996). Direct and long-range action of a wingless morphogen gradient. *Cell* **87**, 833-844.
Zeng, W., Wharton, K. A., Jr, Mack, J. A., Wang, K., Gadbaw, M., Suyama, K., Klein, P. S. and Scott, M. P. (2000). naked cuticle encodes an inducible antagonist of Wnt signalling. *Nature* **403**, 789-795.
Zeng, Y. A., Rahnama, M., Wang, S., Lee, W. and Verheyen, E. M. (2008). Inhibition of Drosophila Wg signaling involves competition between Mad and Armadillo/beta-catenin for dTcf binding. *PLoS ONE* **3**, e3893.
Zhang, J. and Carthew, R. W. (1998). Interactions between Wingless and DFz2 during Drosophila wing development. *Development* **125**, 3075-3085.
Zhang, H., Levine, M. and Ashe, H. L. (2001). Brinker is a sequence-specific transcriptional repressor in the Drosophila embryo. *Genes Dev.* **15**, 261-266.